Carbohydrate Polymers 98 (2013) 1025–1030

Contents lists available at SciVerse ScienceDirect

Carbohydrate Polymers

journal homepage: www.elsevier.com/locate/carbpol

Self-healing guar gum and guar gum-multiwalled carbon nanotubes nanocomposite gels prepared in an ionic liquid

Mukesh Sharma [a], Dibyendu Mondal [a], Chandrakant Mukesh [a], Kamalesh Prasad [a,b,*]

[a] AcSIR-Central Salt & Marine Chemicals Research Institute, G.B. Marg, Bhavnagar, 364002 Gujarat, India
[b] Marine Biotechnology and Ecology Discipline, CSIR-Central Salt & Marine Chemicals Research Institute, G.B. Marg, Bhavnagar, 364002 Gujarat, India

ARTICLE INFO

Article history:
Received 3 June 2013
Received in revised form 25 June 2013
Accepted 28 June 2013
Available online 15 July 2013

Keywords:
Bio-inspired
Ionic liquid
Ion-gel
Carbon nanotube
Self-healing
Bio-adhesive

ABSTRACT

Guar gum is a galactomannan extracted from the seed of the leguminous shrub *Cyamopsis tetragonoloba*. It was found to form a soft viscoelastic gel in 1-butyl-3-methylimidazolium chloride, an ionic liquid at an optimized concentration of 10% w/v. A nanocomposite gel of the gum with enhanced strength could be prepared with 0.2% w/v of multiwalled carbon nanotubes (MWCNTs) in the ionic liquid. When the gels thus prepared were subjected to surface fractures or bisected completely, they found to self-heal at room temperature without any external interventions. The self-healing process could be repeated several times. These viscoelastic gel systems showed thixotropic nature and recovery of the storage modulus with time for several cycles was observed upon rheological investigations. The interaction took place between ionic liquid, guar gum and MWCNT was studied by SEM, TEM, FT-IR, powder XRD and rheometry. The results suggested that, upon standing at room temperature development of electrostatic interactions and the van der Waals interactions among the ionic liquid molecules facilitated the formation of reversible noncovalent bonds and eventually activated the self-healing in the gel systems through appropriate chain entanglements.

© 2013 Elsevier Ltd. All rights reserved.

1. Introduction

Dynamic materials that exhibit reversible properties such as self-healing and superior mechanical properties can be useful for a wide range of applications (Lehn, 2005; Wojtecki, Meador, & Rowan, 2011). Polymer gels show both liquid like flow and elastic behaviour and during their physical interactions solid like properties are obtained. These special properties of the gels make them good candidates to induce functional properties such as self-healing. In recent years, self-healing materials using gels are being developed to increase the durability and lifetime of materials. Among the many approaches to introduce self-repairing ability in gels, one of the popular approaches is the addition of crosslinkers capable of forming reversible crosslinks in the gel network (Urban, 2012). So far, there are many reports of self-healing polymeric gel systems fabricated mainly by crosslinking with groups containing —NH—CO— moiety capable of forming reversible covalent bonds (Hager, Greil, Leyens, Zwaag, & Schubert, 2010; Kushner, Vossler, Williams, & Guan, 2009; Phadke et al., 2012). Imato et al. (2012) have prepared a polymer gel by the reversible formation of diarylbibenzofuranone crosslinker from the dimerization of stable arylbezofuranone, which self-healed without any external stimulus (Imato et al., 2012). Self-healing systems are being designed as inspiration from nature, where any damage caused got self repaired without the intervention of any external stimulus (Urban, 2012). The self-healing systems discussed above involve sharing of electrons leading to formation of covalent bonds and are primarily chemical gel systems. In biological systems, reversible noncovalent molecular interactions play essential roles in the accurate replication of DNA, the folding of proteins into intricate three-dimensional forms and in the detection of molecular signals (Berg, Tymoczko, & Stryer, 2002). Self-healing synthetic systems based on noncovalent interactions depend on the reversible hydrogen bonding or ionic clustering that are visible as reversible crosslinks in polymers (Blaiszik et al., 2010).

In recent years, ionic liquids (ILs) have emerged as unique platform for material design (Lodge, 2008) and also can be used as suitable solvent media for dissolution of many polysaccharides and biopolymers such as DNA (Mukesh, Mondal, Sharma, & Prasad, 2013; Prasad, Izawa, Kaneko, & Kadokawa, 2009; Prasad, Kaneko, & Kadokawa, 2009; Rogers & Seddon, 2003). Moreover, due to the presence of both positive and negative charges, they show electrostatic interactions (Kobrak & Li, 2010). Cation–π interactions are well established between carbon nanotubes and inorganic cations. Further it has been demonstrated that, ILs interact with single walled carbon nanotubes (SWCNTs) through weak van der

* Corresponding author at: Marine Biotechnology and Ecology Discipline, CSIR-Central Salt & Marine Chemicals Research Institute, G.B. Marg, Bhavnagar, 364002 Gujarat, India. Tel.: +91 278 2567760; fax: +91 278 2567562.
E-mail addresses: kamlesh@csmcri.org, drkamaleshp@gmail.com (K. Prasad).

0144-8617/$ – see front matter © 2013 Elsevier Ltd. All rights reserved.
http://dx.doi.org/10.1016/j.carbpol.2013.06.074

Waals interaction along with cation–π interactions (Mpourmpakis, Tylianakis, Papanikolaou, & Froudakis, 2006; Wang et al., 2008a; Wang, Chu, & Li, 2008b). Guar gum (GG) is a galactomannan extracted from the seed of the leguminous shrub *Cyamopsis tetragonoloba* and consists of (1,4)-linked β-D-mannopyranose main chain with branched α-D-galactopyranose unit at the 6-position (Supporting Fig. S1) (Robyt, 1998) and reported to be soluble in BmimCl (Mine, Prasad, Izawa, Sonoda, & Kadokawa, 2010; Prasad et al., 2009a, 2009b).

Although different kinds of interactions have been exploited to design polysaccharide-based physical networks such as hydrogen bonds (Braccini, Rodríguez-Carvajal, & Pérez, 2005), stereo complexion (de Jong et al., 2000), ionic (Chung et al., 2002) or hydrophobic interactions (Tizzotti et al., 2010), host–guest recognition (Charlot, Auzely-Velty, & Rinaudo, 2003) etc. but there is no report on the studies on noncovalent bond triggered self-healing ability of polysaccharide based materials. To introduce noncovalent bonds, chemical modification of the polysaccharide is required to introduce suitable functionalities capable of forming the specific noncovalent interactions. In this article we have studied the self-healing ability in the physical gel systems consisting of GG in BmimCl and in the nanocomposite gel (NC gel) of the gum prepared in the presence on MWCNT (Ind. Patent. Appl. No. 2651/DEL/2012: August 28, 2012). The formation of reversible noncovalent bonds responsible for self-healing did not require any chemical modifications of the polysaccharide unlike the methods reported so far. Further we have studied the interaction taking place between MWCNT, IL and the biopolymer to understand the role of the nanotubes in the self-healing process. There is a report on preparation of stimuli sensitive hydrogel of xanthan derivatives by incorporating N-isopropylacrylamide in to the gel network (Hamcerencu, Desbrieres, Popa, & Riess, 2009). To the best of our knowledge no studies are done so far on self-healing behaviour of the ion gel of GG and its NC gel with MWCNT prepared in ILs.

2. Experimental

2.1. Materials

Guar gum extracted from seeds of *C. tetragonolobus* was purchased from S.D. Fine chemicals, Mumbai, India. The molecular weight was reported to be 4.22×10^6 Da (Rath, Subramanian, Sivanand, & Pradeep, 2001). The sample was purified by Soxhlet extraction with methanol at 80 °C for 3 h and then the dry powder was added to sufficient amount of water and heated to ensure maximum solubility. The thick colloidal mass thus obtained was precipitated in acetone and vacuum dried at 80 °C. The yield of purified guar gum was 96%. The purified gum was used for all the experiments. 1-Butyl-3-methylimidazolium chloride (BmimCl) was procured from Merck & Co., Germany. Multiwalled carbon nanotubes (MWCNT Type 5, OD: 30–50 nm; length: 10–30 μm) was purchased from Sisco Research Laboratories Pvt. Ltd, Mumbai, India and was used as received.

2.2. Preparation of guar gum ion gel

The gelation of GG (10% w/v) was achieved by heating-cooling process (Mine et al., 2010; Prasad et al., 2009a, 2009b). In a typical procedure, GG (0.10 g) was dissolved in BmimCl (1.0 g) by heating at 80–100 °C for 1 h under argon atmosphere (the optimized molar ratio of GG repeating units to BmimCl was 1:27.7). Similarly the nanocomposite gel of GG with MWCNT was prepared by adding 10% of GG in BmimCl containing 0.2% of MWCNT followed by heating at 80–100 °C for 1 h under argon atmosphere. After the respective viscous solutions were cooled to room temperature, it gave formation of the gels. In order to study the interactions among the IL, MWCNT and GG, the respective gels were processed to powder form by adding isopropyl alcohol (IPA) followed by drying.

2.3. Characterizations

The dry samples were placed on carbon coated copper grids (300 mesh sizes) and the transmission electron microscopic (TEM) images of thus prepared samples were obtained using a JEOL transmission electron microscope (Model JEM 2100, Japan) operated at accelerating voltage of 220 kV. The dry samples were dispersed in acetone and coated on aluminium stubs and evaporated to dryness followed by recording of their SEM images on a LEO 1430 VP instrument employing accelerating voltage of 18 kV. FT-IR analyses were recorded on a Perkin Elmer Spectrum GX, FTIR System, USA by taking 2.0 mg of sample in 600 mg of KBr for dry samples and gel/fluid samples as neat. All spectra were averages of two counts with 10 scans each and a resolution of 5 cm^{-1}. Fluorescence spectra were recorded on an Edinburgh F920 (Edinburgh Instrument, UK) fluorescence spectrometer. The thin gel pieces were placed on windows and the spectra were directly obtained by excitation at 260–620 nm (Izawa, Wakizono, & Kadokawa, 2010). Solid state (CP-MAS) NMR was recorded on a Bruker Avance II (500 MHz) spectrometer operated at 125 MHz. Optical micrographs were recorded on a Fine vision optical light microscope, Made in India. Linear viscoelastic properties (controlled deformation mode with 0.01% strain) of gels were carried out on a rheometer (RS1, HAAKE Instruments, Karlsruhe, Germany) using an titanium cone/plate geometry (diameter 60 mm, angle 1° rad, gap 0.052 mm) operating in dynamic mode. All the dynamic rheological data were checked as a function of strain amplitude to ensure that the measurements were performed in the linear viscoelastic region. For thixotropy measurement the shear rates applied were varied from 0 to 1000 s^{-1} of the materials for 60 s in an upward sweep followed by resting of the samples at shear rate 1000 s^{-1} for 30 s and followed up by a downward sweep. The thixotropic area was calculated using Rheowin software. To investigate the time dependent recovery of elastic modulus, G' and loss modulus, G'' were recorded during deformation using strain 1% (linear viscoelastic range) for 300 s at frequency of 1 Hz followed by deformation of the gel employing higher strain (outside linear viscoelastic region) for 100 s at frequency of 1 Hz. The cycle was repeated for ten times for the GG-BmimCl and twelve times for the GG-BmimCl/MWCNT NC gel. The recovery of G' was monitored during the entire deformation–restoration process.

3. Results and discussion

Ion gel in BmimCl with three different concentration of GG (3, 5 and 10% w/v) was prepared by heating–cooling process as described above. The gels were bisected and were kept one upon another or aligned horizontally with each other in close vicinity at room temperature (30 °C). It was observed that, the ion gel with 10% w/v of GG self-healed after 6 h on standing and the gels with 3% of GG was like viscous fluid and leaching out of ionic liquid was observed from the polymer matrices. In the case of 5% w/v GG gel, the gel halves did not self-heal properly as shown in Fig. S2 in the supporting information. Hence the ion gel with 10% w/v GG was considered as optimized gel system showing self-healing ability and termed as GG-BmimCl gel (1) (Fig. 1). The gel was also prepared in presence of 0.2% w/v MWCNT (with respect to BmimCl) and termed as GG-BmimCl/MWCNT NC gel (2) and self-healing of the gel was observed after 5 h on standing at room temperature (Fig. 1). The unified gel structures was again bisected and kept one upon another. The gel pieces self-healed again and the process could be repeated for ten consecutive cycles for GG-BmimCl gel and twelve consecutive cycles for the NC gel. After this, perhaps due to

Fig. 1. Self-healing of bisected (a) guar gum-BmimCl ionic gel and (b) guar gum-BmimCl/MWCNT nanocomposite gel.

the loss of mobility of the IL, the self-healing was not possible. The surface of the gels 1 and 2 were fractured and kept at ambient conditions as shown in Fig. S3 in the supporting information. The gels got self repaired on standing (2.5 h) in case of GG-BmimCl and the time duration was reduced to 2.0 h in case of the NC gel. Further, the reconstituted gels were re-fractured and the restoration of the original gel structure was observed. These cycles could be repeated several times. The well dispersed mixture of MWCNT in BmimCl was placed in isopropyl alcohol (IPA) for 72 h and then IPA was decanted and the residue was vacuum dried to get 3. The gels 1 and 2 were placed in IPA for 72 h and the dry powder thus obtained from the residues were termed as 4 and 5. Prior to the preparation of the GG gel in presence of MWCNT, 0.2% (w/v) MWCNT was added in the IL and ultrasonicated for 20 min. Uniform and stable dispersions of the nanotubes in the ionic liquids were observed under the optical light microscope (supporting Fig. S4). Aggregation of the nanotubes due to the interactions with the ionic liquids was also visible in the micrographs. The formation of interpenetrating networks (IPNs) between GG gel in BmimCl and MWCNT was visible under microscope (supporting Fig. S5). Structurally BmimCl has an electron delocalized 3 centre-4-electron configuration across the N_1—C_2—N_3 (supporting Fig. S1) with a double bond between C_4 and C_5 and weak electron delocalization at centre. C_2 proton is positively charged due to the electron deficiency in the C=N bond and hence attached to the chloride anion, which is basic and negatively charged. Further, cation–π and π–π interactions between IL and carbon nanotubes are well studied (Fukushima & Aida, 2007). Vibrational bands due to C—Cl stretching (894 and 765 cm^{-1}) were shifted to 866 and 761 cm^{-1} in 3 indicated the involvement of the —C^+— of N—C^+—N— in the interaction with the nanotubes. There are minor changes in the vibrational bands due to C=C bond stretching of the nanotubes (hexagonal network) suggesting π–π interactions among them (Fig. 2). The O—H bond stretching of GG was affected by the interaction with the IL indicated formation of hydrogen bonds with the biopolymer (Lacroix, Sultan, Fleury, & Charlot, 2012). Furthermore, presence of weak bands at 804 and 879 cm^{-1} in 5 indicated interaction of the ionic liquid and carbon nanotubes with GG.

The interactions among ILs and MWCNT were further studied by SEM and TEM. The scanning electron micrographs of pure MWCNT showed presence of bundles of nanotubes with average diameter of 30 ± 0.5 nm (Supporting Fig. S6a). The nanotubes became thicker in 3 due to the surface modification of the nanotubes by BmimCl demonstrating interaction of CNT with the IL (Fukushima & Aida, 2007; Wang et al., 2008a, 2008b; Wu et al., 2009) (Supporting Fig. S6b). The increase in thickness of the nanotubes may be due to the presence of ionic liquids on the surface of the nanotubes resulting in aggregation of the tubes. Thick layer formation on carbon nanotubes were observed in 5 indicating attachment of GG on the surface of CNTs (Supporting Fig. S6c).

TEM images of untreated MWCNT showed 9.74 nm inner diameters with 29 concentric walls with diameter 13.91 nm each and clear inner channel (Fig. 3A). The images of 3 in three different locations showed sign of modifications on the concentric walls of the nanotubes. The side walls showed signatures of associative structures and the diameter of both side of the walls have increased

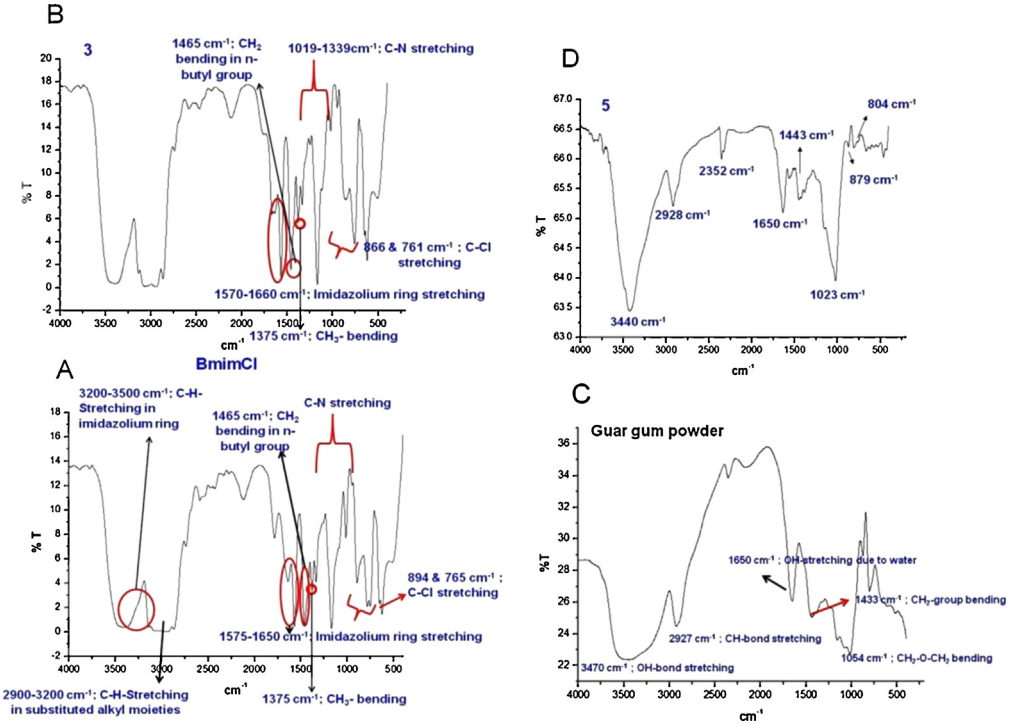

Fig. 2. FT-IR spectra of (A) neat BmimCl, (B) mixture of MWCNT and BmimCl, (C) Guar gum powder and (D) Guar gum-BmimCl/MWCNT nanocomposite gel converted to powder form by treatment with IPA followed by drying.

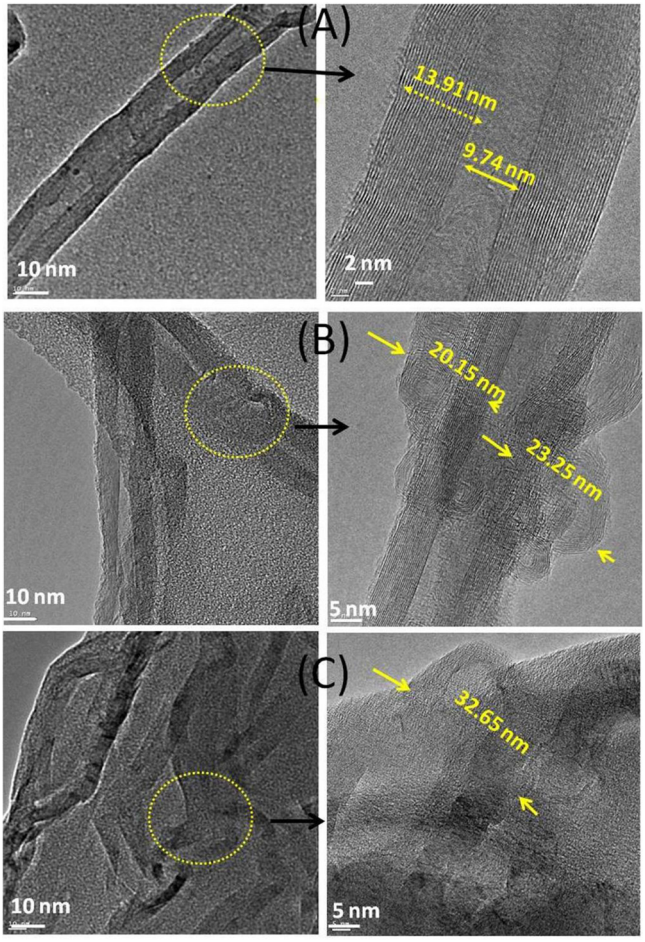

Fig. 3. TEM image of (A) pure MWCNT, (B) BmimCl functionalized MWCNT and (C) interaction of guar gum and BmimCl with MWCNT.

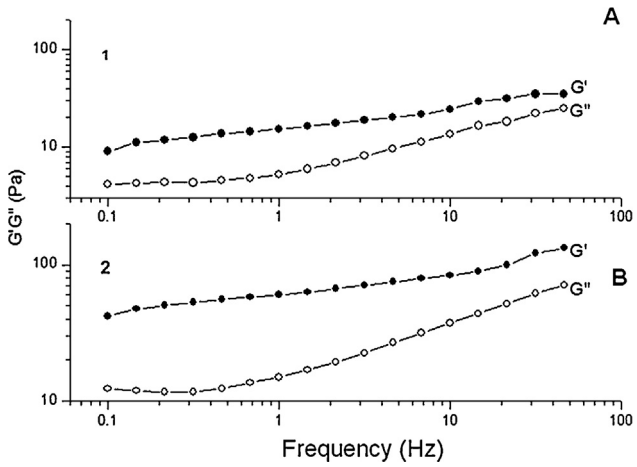

Fig. 4. Evaluation of G' (filled symbols) and G'' (open symbols) moduli as a function of the frequency for (A) guar gum-BmimCl gel and (B) guar gum-BmimCl/MWCNT nanocomposite gel.

to 20.15 and 23.25 nm indicating involvements of the π electron clouds of the CNT in the interaction with the IL (cation–π/π–π) (Fig. 3B). The change in morphology of inner channel of the nanotubes too showed sign of the interactions discussed above. For the sample 4, a more cloudy associative structure on the sidewalls of MWCNT are seen (Fig. 3C). Since the IL forms hydrogen bonds with hydroxyl groups of GG backbone (Lacroix et al., 2012) and hence GG too took part in the interaction process with MWCNT through IL resulting changes in the morphology of the nanotube side walls (Fig. 3C, shown with arrow), where a more cloudy associative structure in comparison to 3 is visible.

Powder X-ray diffraction patterns of MWCNT showed sharper diffraction peaks around 22° and 42° due to crystallinity and GG powder showed broad humps at 19° and 40° due to the intramolecular hydrogen bonding. The crystalline structure of MWCNT was completely disrupted in the gels of 1 and 2 (supporting Fig. S7d and S7e) indicating interaction of IL with GG and carbon nanotubes, which is also evident from FT-IR, SEM and TEM studies discussed above. In case of 5, a sharper peak was observed around 20° indicates washing out of the IL in IPA resulting regeneration of crystallinity. It should be noted that, the original peaks due to MWCNT are not visible indicating strong interactions taking place between GG and MWCNT (supporting Fig. S7c). In addition to this, magic angle spinning solid state ^{1}H and ^{13}C NMR of the 4 and 5 was recorded to further confirm the interactions. In the solid state ^{1}H NMR of 4, a broad peak was observed between 2.34 and 9.54 ppm mostly due to the protons of (1,4)-linked β-D-mannopyranose and 1,6-linked-α-D-galactopyranose of GG (supporting Fig. S8). In these broad peaks the signals of the protons of BmimCl ($NC\underline{H}N$, $CH_3NCHC\underline{H}N$,$CH_3NC\underline{H}CHN$, $NC\underline{H}_2(CH_2)_2CH_3$ and $NC\underline{H}_3$) also merged. The sharp peaks at 0.9 [$N(CH_2)_3C\underline{H}_3$], 1.36 [$N(CH_2)_2C\underline{H}_2CH_3$] and 2.05 [$NCH_2C\underline{H}_2CH_2CH_3$] are due to the alkyl group of BmimCl. The broad peaks observed in 4 became a bit narrow and sharp in 5 indicating disturbance of the structure of (GG in IL) complex due to MWCNT. Two additional broad peaks 7.8 and 9.16 were observed in 5 due to $NC\underline{H}N$, $CH_3NCHC\underline{H}N$, $CH_3NC\underline{H}CHN$ of BmimCl and merging of peaks at 0.9, 1.36, 2.05 of 4 in 5 indicates interaction of MWCNT with IL. In solid state ^{13}C of 5, some additional peaks in comparison to 4 were observed e.g., 13.8, 19.93, 32.78, 37.08, 48.86 and 124.0 further confirming the interactions stated above (supporting Fig. S9). It has been established for cellulose dissolution in ionic liquids that, the anions of IL form strong hydrogen bond with hydroxyl group of cellulose and cations found to be in close contact with polysaccharides through hydrophobic interactions (Liu, Sale, Holmes, Simmons, & Singh, 2010). In case of guar gum, similar interaction with the ILs leads to formation of noncovalent hydrogen bonding.

GG gel in BmimCl has found to show very good fluorescence (Izawa et al., 2010) and the fluorescence quenching by MWCNT is already established (Singh, Iyer, & Giri, 2012). The fluorescence spectra of both the gels 1 and 2 were recorded and the quenching in fluorescence was observed in the gel 2 as shown in supporting Fig. S10 confirming the interaction among GG, CNT and BmimCl established above. It should be noted that, the GG hydrogels did not show the self-healing property due to the absence of the electrostatic interactions in water unlike the ionic liquids (supporting Fig. S11), which further confirmed the crucial role of the interactions triggered by the IL in the self-healing process.

The steady flow behaviour of the gel prepared in presence of MWCNT exhibited much higher shear viscosity in comparison to GG ionic gel indicating formation of stronger gel network. Perhaps the cation–π interactions between BmimCl and MWCNT and the hydrogen bond formation between GG and BmimCl helped the formation of solid like structures through favourable chain entanglements (Supporting Fig. S12). The flow behaviour of both the healed gels was identical to the respective gels before healing suggesting restoration of the mechanical properties of the gels after healing (Supporting Fig. S13). Frequency dependent viscoelastic measurements of the GG-BmimCl and GG-BmimCl/MWCNT NC gel showed signature of typical viscoelastic material with predominance of storage modulus on the whole frequency range (Fig. 4). It should be noted that, the storage modulus was more predominant over the loss modulus in 2 indicating more solid like behaviour for

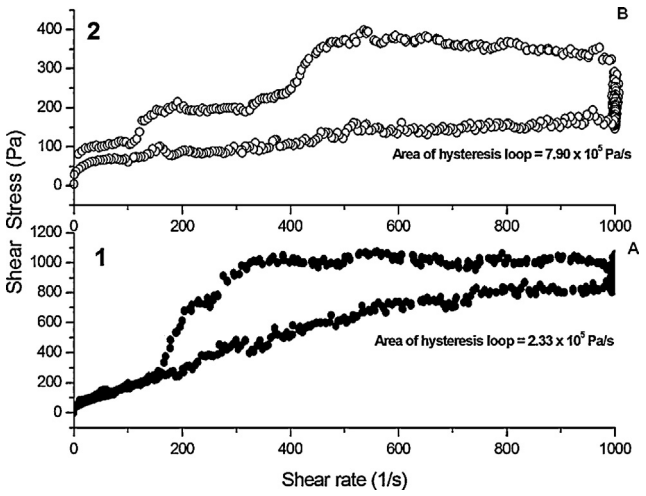

Fig. 5. Evaluation of thixotropic behaviour by hysteresis loop measurements (A) guar gum-BmimCl gel and (B) guar gum-BmimCl/MWCNT nanocomposite gel.

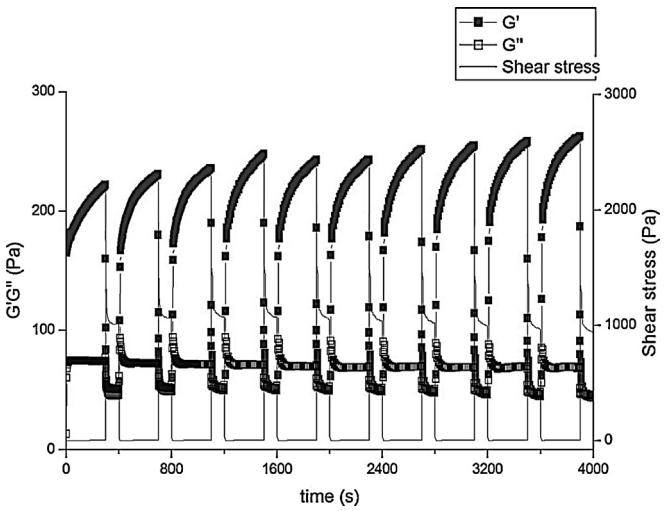

Fig. 6. Self-healing in guar gum-BmimCl gel as characterized by dynamic recovery of the storage modulus (G') upon relaxation.

the NC gel in comparison to the standalone GG ionic gel. Ionotropic gelation involving BmimCl/BmimCl interactions (including Van der Waals and coulombic interactions) and multiple guar gum/BmimCl and hydrogen bonds between guar gum contributed to form a more stable associative system having higher life time of the interactions. The process was further accelerated in the presence of MWCNT. The time dependent viscoelastic response up to 15 min showed dominance of store modulus over loss modulus for both the gels suggesting solid like behaviour of the gels (supporting Fig. S14). In this case also, both the moduli for 2 had higher values in comparison to 1 indicating formation of stronger network structures in the former. BmimCl has a dual functionality since it behaves as a solvent and as a junction promoter that ties guar gum chains, leading to a network structure similar to physical gels. These crosslinkings are not regular but rather form extended junction zones due to the cooperative effect. The three dimensional network upon application of mechanical strain (higher shear rate) was disturbed but upon release of the force reconstitution of the three dimensional structure took place responsible for the self-healing of the gels (Fig. 5). The area of the hysteresis loop formed for the GG-BmimCl gel was 2.33×10^5 Pa/s, which was lower than that of GG-BmimCl/MWCNT (7.9×10^5 Pa/s) explaining the quicker response of the later to mechanical strain towards self-healing. In order to investigate recovery of storage modulus (G') of the gels upon relaxation, the gels were fractured employing high strain followed by relaxation. Each of the gels were initially subjected to 1% strain at 1 Hz frequency for 300 s and G' and G'' were monitored during the process followed by fracturing of the gels employing very high strain at 1 Hz for 100 s. It was observed that, G' of GG-BmimCl gel upon forced deformation recovered to the original value upon relaxation during the deformation–restoration cycles (Fig. 6). The cycles could be repeated for ten consecutive times. The GG-BmimCl/MWCNT NC gel also showed similar restoration of G' with time upon relaxation (Fig. 7) but the cycles could be repeated for twelve consecutive times. The corresponding values of the storage modulus for the later gel were about two fold higher in comparison to the former indicating stronger gel network in the gel and perhaps responsible for the higher degree of stability of the gel under shear. This confirmed the self-healing nature of the gels. Further studies to understand the molecular level interactions leading to self-healing in these novel systems are going on.

For biological systems, development of van der Waals interactions is due to the changes in distribution of electronic charges around an atom with time and the electrostatic interactions among the atoms mainly bring them closer to each other resulting in self-healing (Berg et al., 2002). Likewise, the electrostatic forces as well as the van der Waals interactions in this case played an important role in the self-healing process. In case of GG-BmimCl/MWCNT NC gel the cation–π/π–π interactions between the IL and the carbon nanotubes too plays a key role in the self-repairing. The interactions resulted formation of reversible noncovalent interactions among the bisected gel pieces and were the main driving force for such self repairing.

Apart from showing self-healing property, the gels 1 and 2 showed very good adherence to human finger muscles as shown in supporting Fig. 15 (bio-adhesion). Both the gels found to adhere on finger muscles as long as for 2 h and even after completion of 2 h, the gels found to stick on the finger. But it was felt that, gel 2 had better adhering capability perhaps due to the extra interactions of carbon nanotubes with the building blocks of proteins i.e., amino acids and peptides (Wang & Ai, 2009). In the case of GG gel, the ionic liquid perhaps interacts with protein made it to stick to the finger muscles. Further, it should be noted that, the GG hydrogel did not adhere to human finger muscle, which supports the logic stated above.

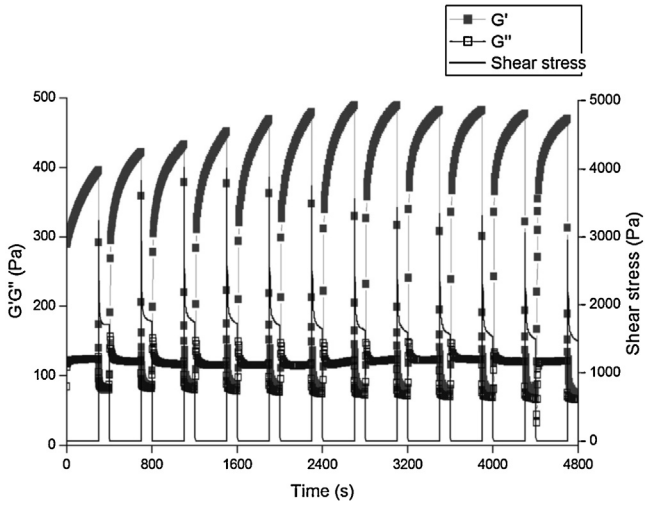

Fig. 7. Self-healing in guar gum-BmimCl/MWCNT nanocomposite gel as characterized by dynamic recovery of the storage modulus (G') upon relaxation.

4. Conclusions

In conclusion, self-healing ability of guar gum gel in BmimCl and its nanocomposite gel with MWCNT is demonstrated. The various experimental results have suggested that, the interaction among the ion pairs of the ionic liquids formed physically crosslinked sites in the ionic gel, which got disturbed upon fracture or bisection of the gels. At room temperature on standing development of the electrostatic interactions as well as the van der Waals interactions among the gel pieces facilitated the formation of reversible non covalent bonds and activated the self-healing process. The noncovalent bond formation on the MWCNT due to the cation–π interactions with the ionic liquids further attributed to the autonomous repair. The thixotropic nature of the gel systems too helped in the formation of reversible non covalent bonds. Furthermore, the gels showed very good adhering property to the human finger muscles. These types of gels may find applications in sensors/actuators and in bio-medical applications. In addition to this polymers and composite materials with the ability to autonomous repair after an induced damage are useful as longer-lasting, fault-tolerant products and components in many applications such as coatings, electronics, transportation, and energy (Burnworth et al., 2011).

Acknowledgements

KP thanks Council of Scientific & Industrial Research, New Delhi for the grant of CSIR-Young Scientist Awardees Project and overall financial support. MS, CM and DM thanks UGC and CSIR for Junior Research Fellowships. Dr. P.K. Ghosh, Director, CSIR-CSMCRI is acknowledged for overall scientific support and constructive suggestions. Discipline of analytical science & centralized instrumentation facility of the institute is gratefully acknowledged for providing all necessary analytical facility for the work.

Appendix A. Supplementary data

Supplementary data associated with this article can be found, in the online version, at http://dx.doi.org/10.1016/j.carbpol.2013.06.074.

References

Berg, J. M., Tymoczko, J. L., & Stryer, L. (2002). Chemical bonds in biochemistry. In *Biochemistry* (5th ed.). New York: W. H. Freeman.

Blaiszik, B. J., Kramer, S. L. B., Olugebefola, S. C., Moore, J. S., Sottos, N. R., & White, S. R. (2010). Self-healing polymers and composites. *Annual Review of Material Research*, *40*, 179–211.

Braccini, I., Rodríguez-Carvajal, M. A., & Pérez, S. (2005). Chain–chain interactions for methyl polygalacturonate: Models for high methyl-esterified pectin junction zones. *Biomacromolecules*, *6*, 1322–1328.

Burnworth, M., Tang, L., Kumpfer, J. R., Duncan, A. J., Beyer, F. L., Fiore, G. L., et al. (2011). Optically healable supramolecular polymers. *Nature*, *472*, 334–337.

Charlot, A., Auzely-Velty, R., & Rinaudo, M. (2003). Specific interactions in model charged polysaccharide systems. *Journal of Physical Chemistry B*, *107*, 8248–8254.

Chung, T. W., Yang, J., Akaike, T., Cho, K. Y., Nah, J. W., Kim, S. I., et al. (2002). Preparation of alginate/galactosylated chitosan scaffold for hepatocyte attachment. *Biomaterials*, *23*, 2827–2834.

de Jong, S. J., de Smedt, S. C., Wahls, M. W. C., Demeester, J., Kettenes-van den Bosch, J. J., & Hennink, W. E. (2000). Novel self-assembled hydrogels by stereocomplex formation in aqueous solution of enantiomeric lactic acid oligomers grafted to dextran. *Macromolecules*, *33*, 3680–3686.

Fukushima, T., & Aida, T. (2007). Ionic liquids for soft functional materials with carbon nanotubes. *Chemistry – A European Journal*, *13*, 5048–5058.

Hager, M. D., Greil, P., Leyens, C., Zwaag, S., & Schubert, U. S. (2010). Self-healing materials. *Advanced Materials*, *22*, 5424–5430.

Hamcerencu, M., Desbrieres, J., Popa, M., & Riess, G. (2009). Stimuli-sensitive xanthan derivatives/N-isopropylacrylamide hydrogels: Influence of cross-linking agent on interpenetrating polymer network properties. *Biomacromolecules*, *10*, 1911–1922.

Imato, K., Nishihara, M., Kanehara, T., Amamoto, Y., Takahara, A., & Otsuka, H. (2012). Self-healing of chemical gels cross-linked by diarylbibenzofuranone-based trigger-free dynamic covalent bonds at room temperature. *Angewandte Chemie International Edition*, *51*, 1138–1142.

Izawa, H., Wakizono, S., & Kadokawa, J. (2010). Fluorescence resonance-energy-transfer in systems of Rhodamine 6G with ionic liquid showing emissions by excitation at wide wavelength areas. *Chemical Communications*, *46*, 6359–6361.

Kobrak, M. N., & Li, H. (2010). Electrostatic interactions in ionic liquids: The dangers of dipole and dielectric descriptions. *Physical Chemistry Chemical Physics*, *12*, 1922–1932.

Kushner, A. M., Vossler, J. D., Williams, G. A., & Guan, Z. (2009). A biomimetic modular polymer with tough and adaptive properties. *Journal of American Chemical Society*, *131*, 8766–8768.

Lacroix, C., Sultan, E., Fleury, E., & Charlot, A. (2012). Functional galactomannan platform from convenient esterification in imidazolium-based ionic liquids. *Polymer Chemistry*, *3*, 538–546.

Lehn, J.-M. (2005). Dynamers: Dynamic molecular and supramolecular polymers. *Progress in Polymer Science*, *30*, 814–831.

Liu, H., Sale, K. L., Holmes, B. M., Simmons, B. A., & Singh, S. (2010). Understanding the interactions of cellulose with ionic liquids: A molecular dynamics study. *Journal of Physical Chemistry B*, *114*, 4293–4301.

Lodge, T. P. (2008). A unique platform for materials design. *Science*, *321*, 50–51.

Mine, S., Prasad, K., Izawa, H., Sonoda, K., & Kadokawa, J. (2010). Preparation of guar gum-based functional materials using ionic liquid. *Journal of Material Chemistry*, *20*, 9220–9225.

Mpourmpakis, G., Tylianakis, E., Papanikolaou, D., & Froudakis, G. E. (2006). A multi scale theoretical study of Li^+ interaction with carbon nanotubes. *Journal of Nanoscience and Nanotechnology*, *6*, 3731–3735.

Mukesh, C., Mondal, D., Sharma, M., & Prasad, K. (2013). Rapid dissolution of DNA in a novel bio-based ionic liquid with long-term structural and chemical stability: Successful recycling of the ionic liquid for reuse in the process. *Chemical Communications*, *49*, 6849–6851.

Phadke, A., Zhang, C., Arman, B., Hsu, C. C., Mashelkar, R. A., Lele, A. K., et al. (2012). Rapid self-healing hydrogels. *Proceedings of the National Academy of Sciences*, *109*, 4383–4388.

Prasad, K., Izawa, H., Kaneko, Y., & Kadokawa, J. (2009). Preparation of temperature-induced shapeable film material from guar gum-based gel with an ionic liquid. *Journal of Material Chemistry*, *19*, 4088–4090.

Prasad, K., Kaneko, Y., & Kadokawa, J. (2009). Novel gelling systems of κ-, ι-, and λ-carrageenans and their composite gels with cellulose using ionic liquid. *Macromolecular Bioscience*, *9*, 376–382.

Rath, R. K., Subramanian, S., Sivanandam, V., & Pradeep, T. (2001). Studies on the interaction of guar gum with chalcopyrite. *Cananadian Metallurgy Quarterly*, *40*, 1–12.

Robyt, J. F. (1998). *Essentials of carbohydrate chemistry*. New York: Springer., 172

Rogers, R. D., & Seddon, K. R. (2003). Ionic liquids-solvents of the future? *Science*, *302*, 792–793.

Singh, D. K., Iyer, P. K., & Giri, P. K. (2012). Role of molecular interactions and structural defects in the efficient fluorescence quenching by carbon nanotubes. *Carbon*, *50*, 4495–4505.

Tizzotti, M., Creuzet, C., Labeau, M. P., Hamaide, T., Boisson, F., Drockenmuller, E., et al. (2010). Synthesis of temperature responsive biohybrid guar-based grafted copolymers by click chemistry. *Macromolecules*, *43*, 6843–6852.

Urban, M. W. (2012). Dynamic materials: The chemistry of self-healing. *Nature Chemistry*, *4*, 80–82.

Wang, J., Chu, H., & Li, Y. (2008). Why single-walled carbon nanotubes can be dispersed in imidazolium-based ionic liquids. *ACS Nano*, *2*, 2540–2546.

Wang, Y., & Ai, H. (2009). Theoretical insights into the interaction mechanism between proteins and SWCNTs: Adsorptions of tripeptides GXG on SWCNTs. *Journal of Physical Chemistry B*, *113*, 9620–9627.

Wang, Z., Zhang, Q., Kuehner, D., Xu, X., Ivaska, A., & Niu, L. (2008). The synthesis of ionic-liquid-functionalized multiwalled carbon nanotubes decorated with highly dispersed Au nanoparticles and their use in oxygen reduction by electrocatalysis. *Carbon*, *46*, 1687–1692.

Wojtecki, R. J., Meador, M. A., & Rowan, S. J. (2011). Using the dynamic bond to access macroscopically responsive structurally dynamic polymers. *Nature Materials*, *10*, 14–27.

Wu, B., Hu, D., Kuang, Y., Liu, B., Zhang, X., & Chen, J. (2009). Functionazation of carbon nanotubes by an ionic liquids polymer: Dispersion of Pt and PtRu nano particles on carbon nano tubes and their electrocatalytic oxidation of methanol. *Angewandte Chemie International Edition*, *48*, 4751–4754.